*JOURNAL OF NANO- AND ELECTRONIC PHYSICS*
Vol. **17** No 4, 04001(6pp) (2025)

*ЖУРНАЛ НАНО- ТА ЕЛЕКТРОННОЇ ФІЗИКИ*
Том **17** № 4, 04001(6cc) (2025)

OPEN ACCESS

## REGULAR ARTICLE

# Modeling the Breakdown of the *p-n* Junction Based on GaAs Using Molecular Dynamics Method

D. Sergeyev[1,2*], N. Zhanturina[2], A.L. Solovjov[3]

[1] *T. Begeldinov Aktobe Avation Institute, 030012 Aktobe, Kazakhstan*
[2] *K. Zhubanov Aktobe Regional University, 030000 Aktobe, Kazakhstan*
[3] *B. Verkin Institute for Low Temperature Physics and Engineering of the National Academy of Sciences of Ukraine, 61103 Kharkiv, Ukraine*

(Received 03 April 2025; revised manuscript received 18 August 2025; published online 29 August 2025)

This paper presents the results of a modeling study of the breakdown of the GaAs-based electron-hole junction using density functional theory and molecular dynamics method. Electrical characteristics were simulated using Slater-Koster and non-equilibrium Green's function methods. It is shown that the presence of initial vacancy defects and Frenkel pairs in the volume of the semiconductor crystal contributes to the relaxation of mechanical stresses created by thermal deformation. It is determined that the electromagnetic component of the pulse leads to the appearance of bends in the semiconductor structure, accompanied by significant deviations of the parameters of the crystal lattice from the norm. When considering the simultaneous action of thermal and electromagnetic components of the pulse, these bends are smoothed out, presumably due to the relaxation of mechanical stresses through initial and thermal vacancy defects. It is revealed that vulnerable areas of the semiconductor device are the junction points of the crystalline structure with the contacts, as well as the boundary between *p*- and *n*-semiconductors. Analysis of electrical characteristics shows that even before the breakdown, the semiconductor diode loses its rectifying properties, and the pre-breakdown state of the diode is accompanied by a significant impulsive in-crease in reverse current, further leading to overheating and thermal breakdown.

**Keywords**: Computer modeling, *p-n* junction, Electromagnetic pulse, Thermal effect, Molecular dynamics.

DOI: 10.21272/jnep.17(4).04001 PACS numbers: 07.05.Tp, 73.40. – c, 31.15. – p

## 1. INTRODUCTION

It is known that powerful electromagnetic pulses (PEMP), arising both unintentionally (naturally) and intentionally (artificially), disrupt the normal functioning of radio-electronic equipment (REE) and either cause temporary deterioration in performance or complete cessation of the required function [1, 2]. Functional impairments of REE can manifest as false triggers; malfunctions in important nodes and modules; distortion of signal shapes at the output; unauthorized activations of executive modules, etc. [3]. The work [4] demonstrates that sources of ultra-wideband (UWB) electromagnetic pulses (EMP) pose a significant threat to modern REE. It should be noted that according to standard [5], UWB EMP are impulse electromagnetic fields of non-nuclear origin with parameters of percent bandwidth greater than 25, electric field amplitude of 100 V/m or more, and frequency range from hundreds of MHz to several GHz.

The most vulnerable electronic components to PEMP exposure are semiconductor devices [6]. When external PEMP affects the operability of REE, the disturbances are primarily accompanied by irreversible physical processes in semiconductor devices, associated with the breakdown of the structure of the electron-hole junction or metal-conductor junction (in Schottky devices), etc. Common damages to semiconductor devices in REE occur due to thermal breakdown, which depending on the type of electronic devices, manifest as surface breakdown, bulk breakdown, dielectric breakdown, through breakdown in transistors with multiple junctions.

Currently, there is widespread discussion about the development of aviation bombs that generate UWB PEMP similar to a nuclear explosion, where conventional chemical explosives are used instead of nuclear material [7]. It is also worth noting that one of the most common variants of EMP bombs is the use of a flux compression generator and a virtual cathode generator [8]. The widespread use of semiconductor materials in almost all industries, which ensure the normal functioning of human life, makes such weapons extremely effective.

One of the important semiconductor materials, third in terms of industrial usage scale (after common semiconductors such as silicon Si and germanium Ge), and until the 1990s predominantly used in the military

* Correspondence e-mail: serdau@mail.kz





Cite this article as: D. Sergeyev et al., *J. Nano- Electron. Phys.* 17 No 4, 04001 (2025) https://doi.org/10.21272/jnep.17(4).04001

industry, is the compound of gallium Ga and arsenic As-gallium arsenide (GaAs). It is known that to assess the state of such semiconductor structures under the influence of PEMP, thermal, electrothermal, electrical, ionization-doping models are used [9]. These models have specific areas of application and are not without their drawbacks. This work is dedicated to the model study of the breakdown of the electron-hole junction based on GaAs. The application of atomistic methods to study the interaction of PEMP with matter allows for the exploration of mechanisms of thermal deformation and destruction, as well as modeling all stages of EMP interaction with the condensed phase.

## 2. SIMULATION MODEL AND METHODS

The simplified geometric model of the GaAs-based electron-hole junction is depicted in Fig. 1. The electron-hole junction model consists of 52 layers of GaAs, half of which are doped with electrons (indicated by blue background in the figure), while the other half are doped with holes (indicated by red background in the figure). The concentration of electrons and holes varies depending on the type of semiconductor from $10^{13}$ см$^{-3}$ to $2 \times 10^{15}$ см$^{-3}$. The optimization of the geometric parameters of the semiconductor structures was carried out within the framework of density functional theory with generalized gradient approximation (GGA), where atomic configurations were relaxed until the forces on all atoms fell below the specified threshold value of 0.05 eV/Å. The right and left electrodes extend the semiconductor structure with a length of approximately 11.307 Å.

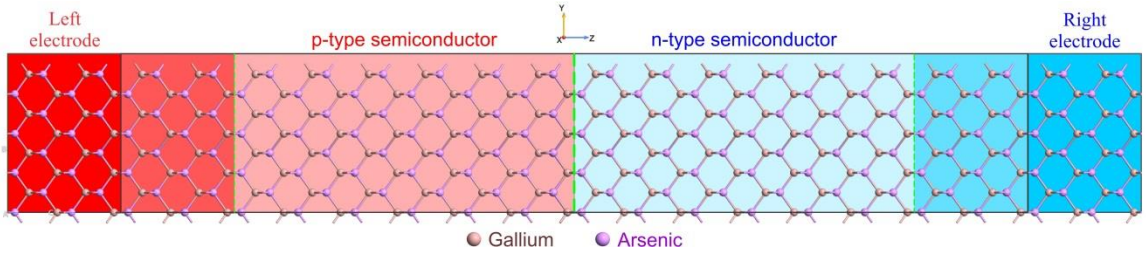


**Fig. 1** – Simplified geometric model of the GaAs-based electron-hole junction

To model the process of semiconductor structure breakdown, a classical molecular dynamics method [10, 11] was employed. To describe the evolution of the structure consisting of $N$ interacting atoms, the system of Newton's equations [12] is utilized:

$$m_i \frac{d^2\mathbf{r}_i(t)}{dt^2} = \mathbf{F}_i\left[\mathbf{r}_1, \ldots, \mathbf{r}_N\right] \quad (1)$$

or taking into account $\frac{d\mathbf{r}_i(t)}{dt} = \mathbf{v}_i(t)$

$$m_i \frac{d\mathbf{v}_i(t)}{dt} = \mathbf{F}_i\left[\mathbf{r}_1, \ldots, \mathbf{r}_N\right] \quad (2)$$

where $m_i$, $\mathbf{r}_i$ and $\mathbf{v}_i$ – mass, coordinate and velocity of the $i$-th particle ($i = 1, \ldots, N$), $\mathbf{F}_i$ – force, acting on $i$-th particle. By solving the system of equations 1, 2, it is possible to determine the trajectory of interacting atoms (particles) as well as analyze the temporal evolution of the system. Potentials Tersoff_GaAs_2011 [13] and Tersoff_GaAs_2002 [14] were chosen to describe Ga and As atoms.

The current-voltage characteristics (CVC) of the electron-hole junction were determined within the framework of the Slater-Koster method combined with the Non-Equilibrium Green's Functions (NEGF) method (SK+NEGF) [15, 16]. The semi-empirical Slater-Koster method was adjusted for calculating the electrical characteristics of the junction as follows: a $k$-point grid of (7, 7, 100) was chosen, and the Bassani. GaAs basis set was selected [17]. When calculating the CVC, the bias voltage was selected in the range from – 2 V to 2 V, and the energy from – 2 eV to 2 eV, with a $k$-point grid of 21 × 21. The calculation of the CVC of the $p$-$n$ junction was performed within the Landauer formalism:

$$I(V_L, V_R, T_L, T_R) = \frac{2e}{h}\int_{-\infty}^{+\infty} T(\varepsilon)\left[f\left(\frac{\varepsilon-\mu_R}{k_B T_R}\right) - f\left(\frac{\varepsilon-\mu_L}{k_B T_L}\right)\right] d\varepsilon \quad (3)$$

where $e$ is the electron charge, $h$ is the Planck constant, $f(\varepsilon)$ is the Fermi energy distribution function of quasiparticles, $k_B$ is the Boltzmann constant, $T_L$, $T_R$ are the current temperatures and $\mu_R$, $\mu_L$ are the electrochemical potentials of the right and left electrodes. The simulation of the electric transport properties of the p-n junction was implemented in the Atomistix ToolKit with Virtual NanoLab program. The OriginPro program was used to process the obtained numerical data.

The fundamental equations of these methods are elaborated in more detail in works [18, 19].

## 3. RESULTS AND DISCUSSION

It is known that one of the main destructive factors of semiconductor structures under the influence of EMP is thermal deformation (thermal compression and expansion). Let's consider the obtained results of the model destruction of the GaAs $p$-$n$ junction: a) taking into account only thermal effects; b) taking into account only electromagnetic effects; c) taking into account simultaneous effects of thermal and electromagnetic components of EMP.

As can be seen, the destruction of the p-n structure occurs through high-speed thermal deformation (Fig. 2). At the initial stage (at $t \approx 7$ ps), there is a thermal displacement of Ga and As atoms from the lattice site to the interstitial site, creating "thermal" Frenkel defect pairs. Thus, the process of defect generation in a defect-free crystal occurs due to thermal compression or expansion.

For a silicon junction, the process of thermal deformation began at a temperature of 460 K [20], while for the GaAs junction under consideration, it is observed at 700 K. Further retention of the semiconductor structure at this temperature leads to an increase in the concentration of various defects and their coagulation (clustering). Subsequently, at $t \approx 7.9$ ps, the structure collapses at the site of defect clustering, accompanied by a rapid increase in the kinetic energy of quasi-particles.

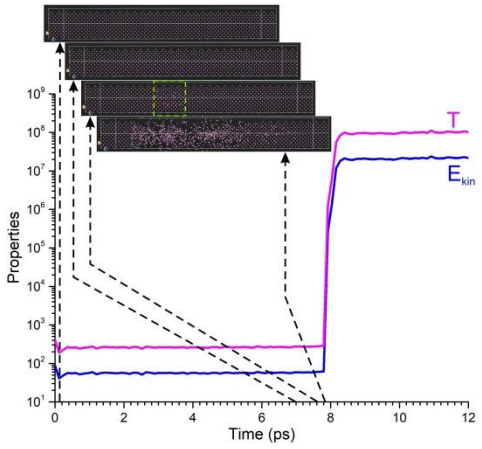


**Fig. 2** – Destruction of the electron-hole junction (Temperature and kinetic energy change over time)

If the temperature pressure ceases in the pre-destructive state, the structure of the junction relaxes, i.e., with a low degree of thermal deformation, elastic compression is observed. The lattice relaxation occurs with the annihilation of excess defects formed. It is noted that theoretically, for irreversible displacement of a Ga or As atom, it is sufficient to overcome half of the interatomic bonds, which is ~ 2.83 Å.

The evolution of the destruction of the *p-n* structure with initial vacancy defects is shown in Fig. 3.

The defect plane is marked with a green arrow. At $t \approx 10.90$ ps, noticeable displacement of Ga and As atoms is observed in the area of the *n*-type semiconductor, although the initial vacancy defects are in the *p*-type semiconductor area. At $t \approx 11$ ps, defect clustering occurs, and the beginning of the structure detachment.

The onset of semiconductor structure destruction is observed in the defect-free region (in this case, in the *n*-type semiconductor area, while the defective region is in the p-type semiconductor) at 10.9 ps. Destruction at the defective site occurs 11.12 ps later as a continuation of the destructive process. Logically, it would be correct if the destruction of the semiconductor started at the weakened site (in the defective region), as it is precisely in this area that the material's

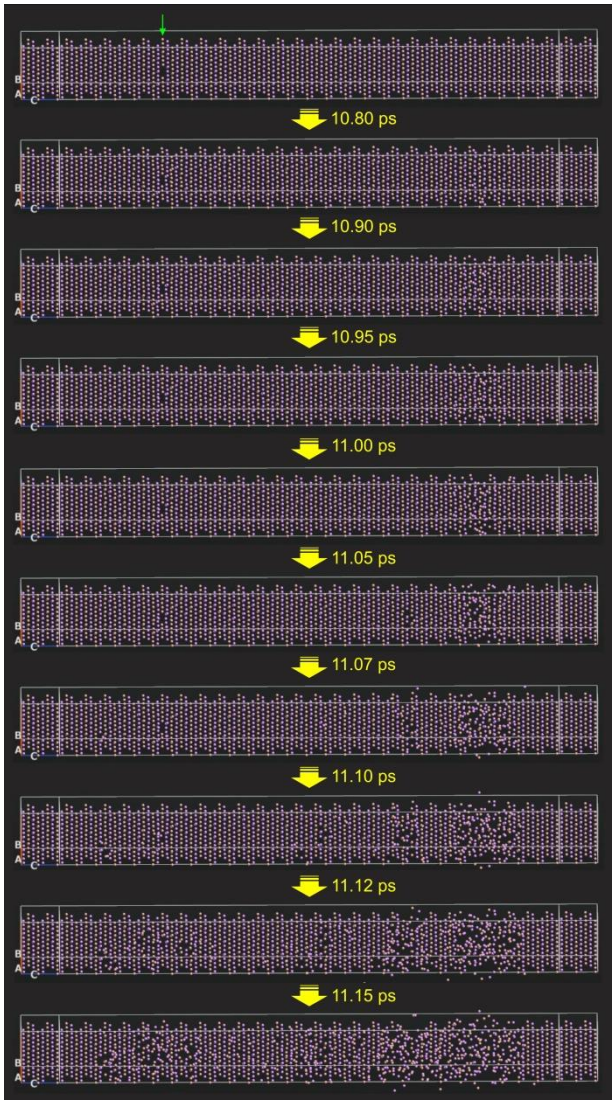


**Fig. 3** – The evolution of the destruction of the electron-hole junction with the presence of initial vacancy defects

strength is significantly reduced. However, the destruction starts in the defect-free part of the crystal. It is likely that the presence of a small concentration of defects leads to the relaxation of mechanical stresses arising from thermal deformation, which restrains the overheating and destruction process. It is noted that at the same moment, destruction occurs at the contact point (at the interface) of the *p*- and *n*-semiconductors.

Purely for the theoretical determination of the impact of the electromagnetic component of the pulse on the change in the semiconductor structure, let's consider the process of EMP impact without taking into account the influence of thermal overheating (Fig. 4).

It should be noted that when EMP is applied, thermal overheating of the structure undoubtedly occurs, as part of the EMP energy is dissipated into Joule heating $\varepsilon = \frac{1}{m}\int_0^t IUdt$ (here, $m$ is the sample mass, $I$ is the current

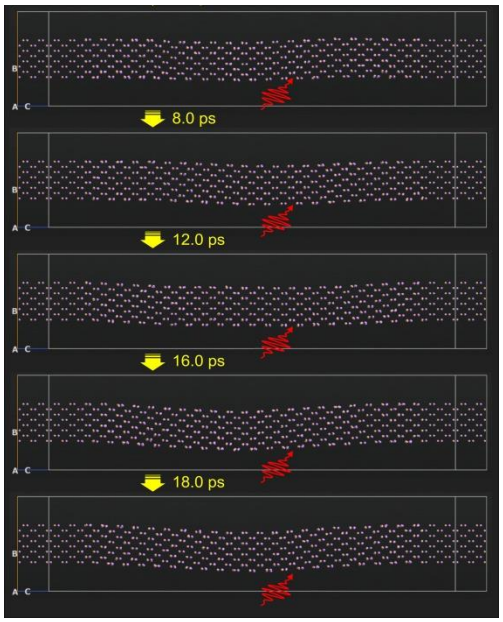


**Fig. 4** – The influence of the electromagnetic component of the pulse on the semiconductor structure


**Fig. 5** – The evolution of the destruction of the *p-n* junction under simultaneous influence of the thermal and electromagnetic components of the pulse

passing through the sample, $U$ is the active component of the voltage across the sample), and some portion of the EMP energy is absorbed by the lattice. (The active component of the voltage is determined by the formula $U = u - L\frac{dI}{dt}$, here $u$ is the voltage on the semiconductor sample, $L$ is the inductance). As can be seen, deformation of the p-n structure is observed. The central region of the junction undergoes significant deformation, bending of the structure is observed, which intensifies over time and leads to a substantial deviation of the lattice parameter of the structure (the lattice parameter varies from 5.653 Å to 5.588 Å). At 18 ps, the deviation of the lattice parameter varies from 5.54 Å to 6.11 Å. Note that the amplitude of the EMR effect on the semiconductor structure varied from $10^5$ V to $10^6$ V.

The evolution of the junction destruction under simultaneous exposure to electromagnetic and thermal components of the EMP is presented in Fig. 5.

Destruction occurs faster than without considering the electromagnetic component. At 2.5 ps, a wave-like deformation of the structure is observed in the middle of the junction. Subsequently, at 3.1 ps, atom displacement near the right electrode begins, possibly causing the wave-like deformation to disappear distinctly. Chaotic coagulation of atoms occurs near the right electrode at 7.85 ps, and at the same location, structure destruction begins at 7.6 ps.

The destruction of the p-n structure with vacancy defects, considering the impact of both electromagnetic and thermal components of the EMP, is shown in Fig. 5. (The defective plane is marked with a green arrow.)

Strong bends, resulting from the interaction of the crystal with the electromagnetic field, are smoothed out under the simultaneous influence of the thermal and electromagnetic components of the EMP. Presumably, this smoothing is associated with the relaxation of the mechanical stresses arising from the initial vacancy defects.

Comparison of the CVC of the model GaAs-based *p-n* junction in the working and pre-destructive states is presented in Fig. 7 (the CVC of the working model diode is indicated by the red curve, the CVC in the pre-destruction state of the p-n junction by the blue curve, the CVC at the beginning of the destruction stage of the p-n junction by the green curve). CVC of the p-n junction under consideration was calculated using Eq. (3). As can be seen, even in the pre-destructive state, the diode completely loses its rectifying properties. The onset of the pre-destructive state of the diode is accompanied by a sharp increase in reverse current. This is explained by the emergence of ionization current, coinciding in direction with the saturation current of the *p-n* junction. Subsequently, the ionization current stimulates overheating of the semiconductor structure, which will lead to thermal breakdown and failure of the diode.

## 4. CONCLUSION

Thus, in this study, molecular dynamics simulation of the *p-n* junction destruction process based on GaAs was conducted using the Theory of Density Functional. The evolution of semiconductor structure destruction by thermal and electromagnetic deformation was demonstrated. It was shown that the presence of initial point defects

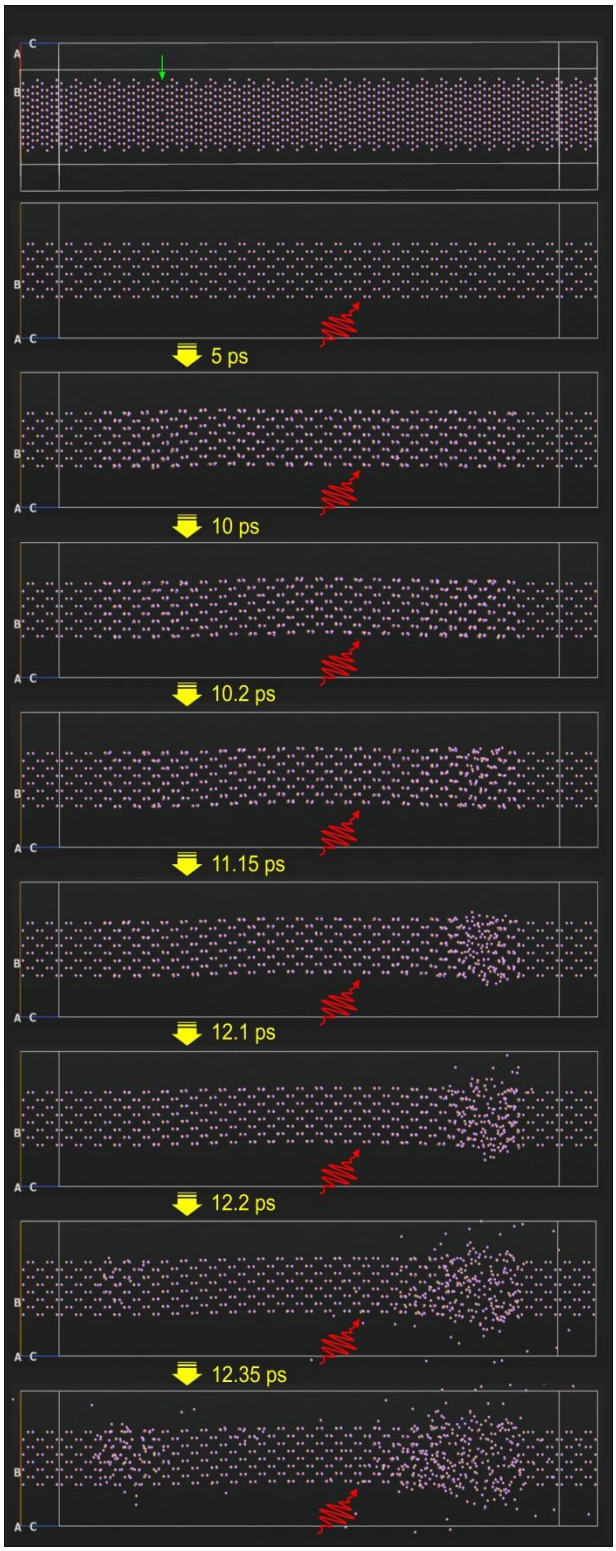


**Fig. 6** – The evolution of the destruction of the *p-n* junction with initial vacancy defects under simultaneous influence of the thermal and electromagnetic components of the pulse

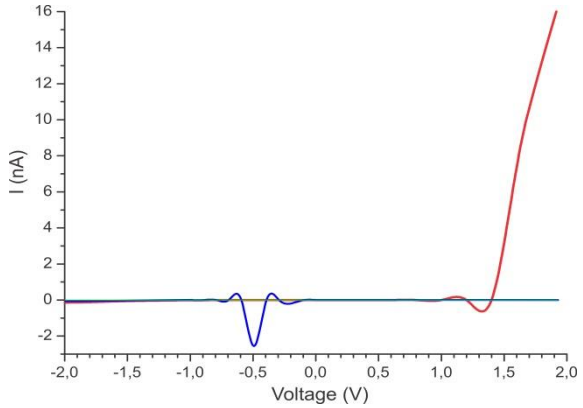


**Fig. 7** – The CVC of the electron-hole junction (the CVC of the working model diode is indicated by the red curve, the CVC in the pre-destruction state of the *p-n* junction by the blue curve, the CVC at the beginning of the destruction stage of the *p-n* junction by the green curve)

(such as vacancies or Frankel defect pairs) leads to the relaxation of mechanical stresses arising from thermal deformation, which delays the overheating process for some time. It was established that the electromagnetic component of the pulse leads to a significant deviation of the GaAs lattice parameter (varying from 5.54 Å to 6.11 Å) and the appearance of structures in the form of bends; however, noticeable bends are smoothed out under the simultaneous influence of thermal and electromagnetic components of the pulse due to the relaxation of mechanical stresses caused by vacancy defects. Vulnerable areas of the junction were identified as the junctions of the semi-conductor structure to contacts, as well as the boundary between *p*- and *n*-semiconductors. It was demonstrated that in the pre-destructive state, the diode completely loses its rectifying properties, and the onset of the pre-destructive state of the diode is accompanied by a significant impulsive increase in reverse current, leading to severe overheating and thermal breakdown.

The obtained results can be useful in developing testing methodologies for semiconductor structures' resistance to external electromagnetic pulse effects, as well as in conducting activities aimed at improving the reliability and stability of semiconductor devices.

## ACKNOWLEDGEMENTS

This work was supported by grant of the Ministry of Science and Higher Education of the Republic of Kazakhstan AP23488734.

## REFERENCES


1. S. Gao, E. Cheng, Y. Chen, Y. Wang, *J. Phys.: Conf. Ser.* **1325**, 012165 (2019).
2. D. Kumar, N.R. Prakash, S. Singh, *IEEE International Conference on Electromagnetic Interference and Compatibility,* 69 (2015).
3. W.-Y. Yin, X.T. Dong, J. Mao, L-W. Li, 17th *International Zurich Symposium on Electromagnetic Compatibility*, 445 (2006).
4. S. Frank, L.M. Eric, *Ultra-Wideband, Short-Pulse Electromagnetics* **10** (2014).
5. IEC 61000-2-13 Electromagnetic compatibility (EMC) – Part 2-13: Environment-High-power electromagnetic (HPEM) environments – Radiated and conducted (2005) (webstore.iec.ch/publication/4131).
6. M. Miao, Y. Zhou, A.J. Salcedo, J.-J. Hajjar, J.J. Liou, *IEEE Electron Dev. Lett.* **37** No 11, 1477 (2016).
7. M. Abrams, *IEEE Spectrum* **40** No 11, 24 (2003).
8. G.M. Banjac, V.D. Dordevic, M.Z. Zivkovic, A. Ferdjali, *Military Technical Courier* **69** No 2, 499 (2021).
9. *Review of Quality and Reliability Handbook*, NEC Electronic corp. (2023).
10. M. Ben-Nun, T.J. Martinez, *Adv. Chem. Phys.* **121**, 439 (2002).
11. Wm.G. Hoover, *Molecular Dynamics* (Springer Berlin, Heidelberg: 2013).
12. A.Y. Kuksin, G.E. Norman, V.V. Stegailov, A.V. Yanilkin, P.A. Zhilyaev, *Int. J. Fracture* **162** No 1-2, 127 (2010).
13. K.A. Fichthorn, Y. Tiwary, T. Hammerschmidt, P. Kratzer, M. Scheffler, *Phys. Rev. B* **83**, 195328 (2011).
14. K. Albe, K. Nordlund, J. Nord, A. Kuronen, *Phys. Rev. B* **66**, 035205 (2002).
15. M.D. Ganjia, F. Nourozi, *Physica E* **40**, 2606 (2008).
16. D. Sergeyev, *J. Nano- Electron. Phys.* **12** No 3, 03017 (2020).
17. J.-M. Jancu, R. Scholz, E.A. de Andrada e Silva, G.C. La Rocca, *Phys. Rev. B* **72**, 193201 (2005).
18. D. Sergeyev, A. Duisenova, A. Solovjov, N. Ismayilova, *Res. Phys.* **54**, 107140 (2023).
19. D. Sergeyev, *Adv. Nano Res.* **10** No 4, 339 (2021).
20. D. Sergeyev, K. Shunkeyev, N. Zhanturina, A.L. Solovjov, *J. Nano- Electron. Phys.* **15** No 4, 04033 (2023).


## Моделювання пробою *p-n* переходу на основі GaAs з використанням методу молекулярної динаміки


Д. Сергєєв[1,2], Н. Жантуріна[2], А.Л. Соловйов[3]

[1] *Актюбінський авіаційний інститут імені Т. Бегельдінова, 030012 Актобе, Республіка Казахстан*
[2] *Актюбінський регіональний університет імені К. Жубанова, 030000 Актобе, Республіка Казахстан*
[3] *Фізико-технічний інститут низьких температур ім. Б. Веркіна НАН України, 61103 Харків, Україна*



У цій статті представлені результати моделювання пробою електронно-діркового контакту на основі GaAs з використанням теорії функціоналу густини та методу молекулярної динаміки. Електричні характеристики моделювалися за допомогою методів Слейтера-Костера та нерівноважних функцій Гріна. Показано, що наявність початкових вакансійних дефектів та пар Френкеля в об'ємі напівпровідникового кристалу сприяє релаксації механічних напружень, що створюються термічними деформаціями. Визначено, що електромагнітна складова імпульсу призводить до появи вигинів у напівпровідниковій структурі, що супроводжуються значними відхиленнями параметрів кристалічної решітки від норми. При розгляді одночасної дії теплової та електромагнітної складових імпульсу ці вигини згладжуються, ймовірно, через релаксацію механічних напружень через початкові та теплові вакансійні дефекти. Виявлено, що вразливими ділянками напівпровідникового приладу є точки з'єднання кристалічної структури з контактами, а також межа між *p*- та *n*-напівпровідниками. Аналіз електричних характеристик показує, що ще до пробою напівпровідниковий діод втрачає свої випрямні властивості, а передпробійний стан діода супроводжується значним імпульсним збільшенням зворотного струму, що надалі призводить до перегріву та теплового пробою.



**Ключові слова**: Комп'ютерне моделювання, *p-n* перехід, Електромагнітний імпульс, Тепловий ефект, Молекулярна динаміка.